

Supporting information

to

## Inhibition of amyloid $\beta$ -induced lipid membrane permeation and amyloid $\beta$ aggregation by K162

Dusan Mrdenovic,<sup>†,§</sup> Piotr Zarzycki,<sup>#</sup> Marta Majewska,<sup>†</sup> Izabela S. Pieta,<sup>†</sup> Robert Nowakowski,<sup>†</sup> Włodzimierz Kutner,<sup>†,‡</sup> Jacek Lipkowski,<sup>§</sup> Piotr Pieta<sup>†,\*</sup>

<sup>†</sup>Institute of Physical Chemistry, Polish Academy of Sciences, Kasprzaka 44/52, 01-224 Warsaw, Poland

<sup>§</sup>Department of Chemistry, University of Guelph, 50 Stone Road East, Guelph, Ontario N1G 2W1, Canada

<sup>#</sup>Energy Geosciences Division, Lawrence Berkeley National Laboratory, 1 Cyclotron Road, Berkeley, California, United States

<sup>‡</sup>Faculty of Mathematics and Natural Sciences, School of Sciences, Cardinal Stefan Wyszyński University in Warsaw, Wóycickiego 1/3, 01-815 Warsaw, Poland

Corresponding author e-mail address:

[ppieta@ichf.edu.pl](mailto:ppieta@ichf.edu.pl)

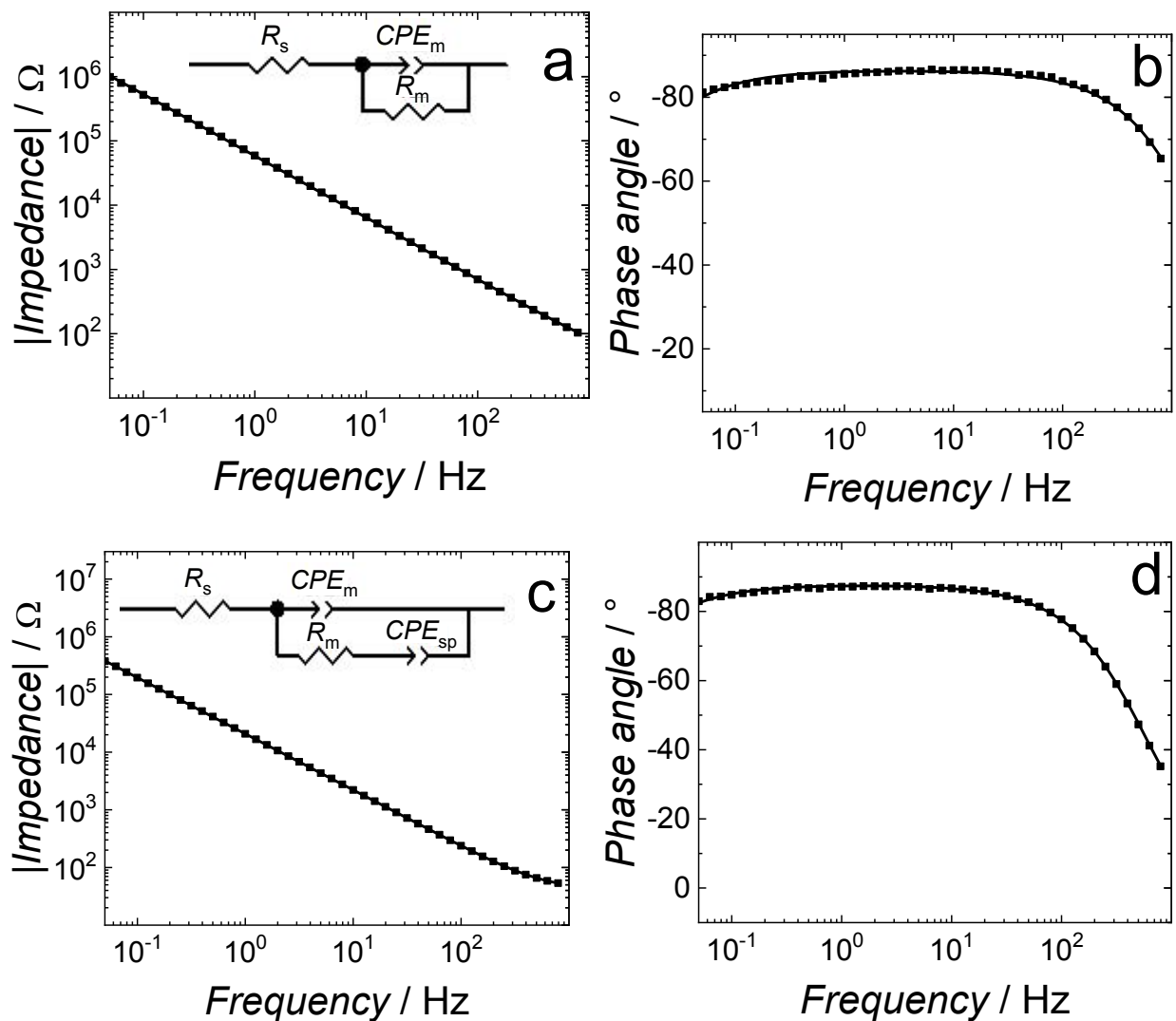


**Figure S1.** (a, c) Impedance and (b, d) phase angle as a function of frequency for (a, b) BLM, (c, d) BLM-A $\beta$ Os-K162 (externally added) in the PBS (0.01 M phosphate buffer, 0.0027 M KCl, and 0.137 M NaCl, pH = 7.4) solution at 0 V vs. SCE. Symbols and lines of the same colors represent experimental data and results of fitting of parameters of the equivalent electrical circuits to the EIS data, respectively, for the same measurement at a single potential. The equivalent electric circuit, shown in Panel (a), was fitted to the EIS data for BLM, BLM-A $\beta$ Os-K162PI, and BLM-A $\beta$ Os-K162EA, while the equivalent electric circuit, shown in Panel (c), was fitted to EIS data for BLM-A $\beta$ Os.

**Table S1.** Numerical results of the equivalent electric circuits fittings to the EIS data for the BLM in the absence of both A $\beta$ Os and K162 (BLM), BLM in the presence of A $\beta$ Os (BLM-A $\beta$ Os), BLM-A $\beta$ Os in the presence of pre-incorporated K162 (BLM-A $\beta$ Os-K162PI), and BLM-A $\beta$ Os in the presence of externally-added K162 (BLM-A $\beta$ Os-K162EA) at 0 V vs. SCE in the PBS (0.01 M phosphate buffer, 0.0027 M KCl, and 0.137 M NaCl, pH = 7.4) solution.

Membrane	$Q_m / \mu\text{F cm}^{-2}$	$\alpha$	$R_m / \text{M}\Omega \text{ cm}^2$	$Q_{sp} / \mu\text{F cm}^{-2}$	$\alpha_{sp}$
BLM	3.72 $\pm$ 0.01	0.96 $\pm$ 0.01	7.25 $\pm$ 0.41	/	/
BLM-A $\beta$ Os	11.57 $\pm$ 0.05	0.97 $\pm$ 0.01	0.079 $\pm$ 0.005	2.47 $\pm$ 0.05	0.796 $\pm$ 0.007
BLM-A $\beta$ Os-K162 (K162 pre-incorporated)	11.79 $\pm$ 0.01	0.96 $\pm$ 0.001	0.954 $\pm$ 0.011	/	/
BLM-A $\beta$ Os-K162 (K162 externally added)	10.19 $\pm$ 0.01	0.97 $\pm$ 0.01	3.29 $\pm$ 0.1	/	/

$Q_m$  – membrane capacitance,  $\alpha$  - an empirical constant related to the frequency dispersion,  $R_m$  – membrane resistance,  $Q_{sp}$  – capacitance of the spacer region (SAM-Tg)

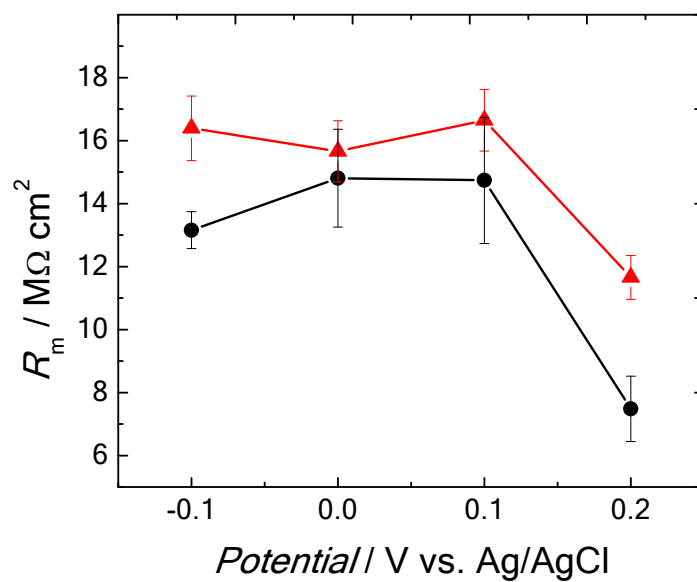


**Figure S2.** Two independent measurements of the membrane resistance ( $R_m$ ) as a function of applied potential in the PBS (0.01 M phosphate buffer, 0.0027 M KCl, and 0.137 M NaCl, pH = 7.4) solution.

Morphology of the BLM deposited and imaged immediately after high-temperature preparation of the lipid vesicle solution is shown in Figure S2a. This BLM consists of two domains with a thickness difference of  $\sim 1$  nm (Figure S2b). The BLM mostly consists of DSPE and DPPC molecules (50% and 15%, respectively) with a 74 °C and 41 °C, respectively, melting temperature.<sup>1,2</sup> The vesicle solution prepared at 50 °C incurs the DPPC phase transition from the gel to the liquid crystalline phase in which acyl chains are melted, thus producing in the BLM a thinner ( $\sim 5$  nm thick) domain. Under these conditions, DSPE remains in the gel phase, where acyl chains are fully extended, to make it thicker ( $\sim 6$  nm).

Domains of lipids in different phases (Figure S2a) are significantly larger than the small domains formed in the gel phase BLM (Inset in Figure 2a). Moreover, the thickness difference between small domains is  $\sim 0.3$  nm (Inset in Figure 2a), which is significantly smaller than that of lipid domains in the gel and liquid crystalline phases (Figure S2). Phase diagrams for mixed lipid bilayers composed of distearoylphosphatidylcholine (DSPC), dioleoylphosphatidylcholine (DOPC), and Chol are reported.<sup>3–5</sup> At Chol mole fraction of  $\sim 0.4$ – $0.7$ , a single-phase BLM is formed in which lipids are clustered into nanodomains. Although different lipids were used in the present study, the Chol concentration was the same as in the former studies.<sup>3–5</sup> Therefore, small domains formed in the gel phase BLM are identified as lipid clusters (Figure 2a).

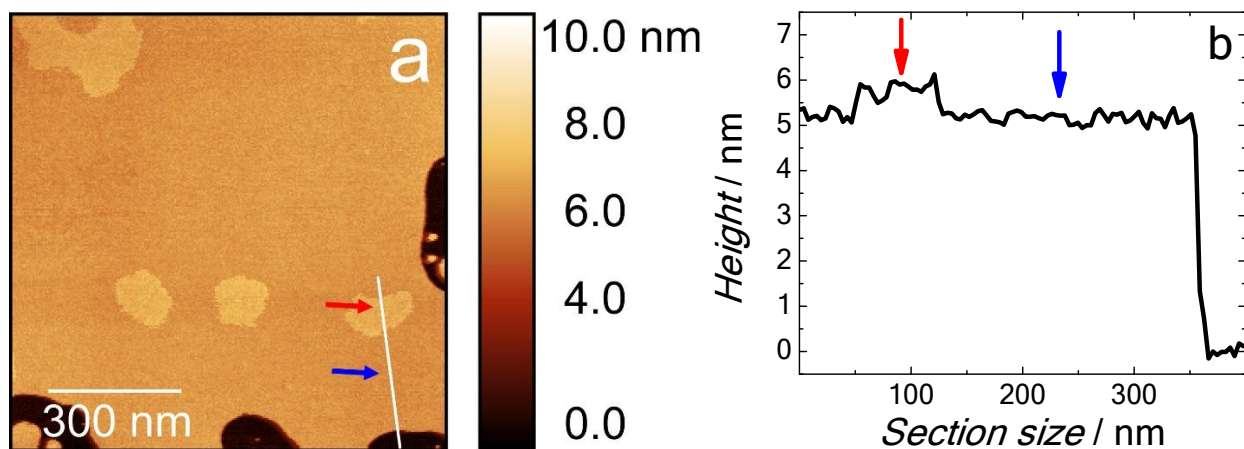


**Figure S3.** (a) The AFM image and (b) the corresponding cross-sectional profile of the BLM, deposited on a mica substrate immediately after lipid vesicle solution preparation. The BLM was imaged in the PBS (0.01 M phosphate buffer, 0.0027 M KCl, and 0.137 M NaCl, pH = 7.4) solution.

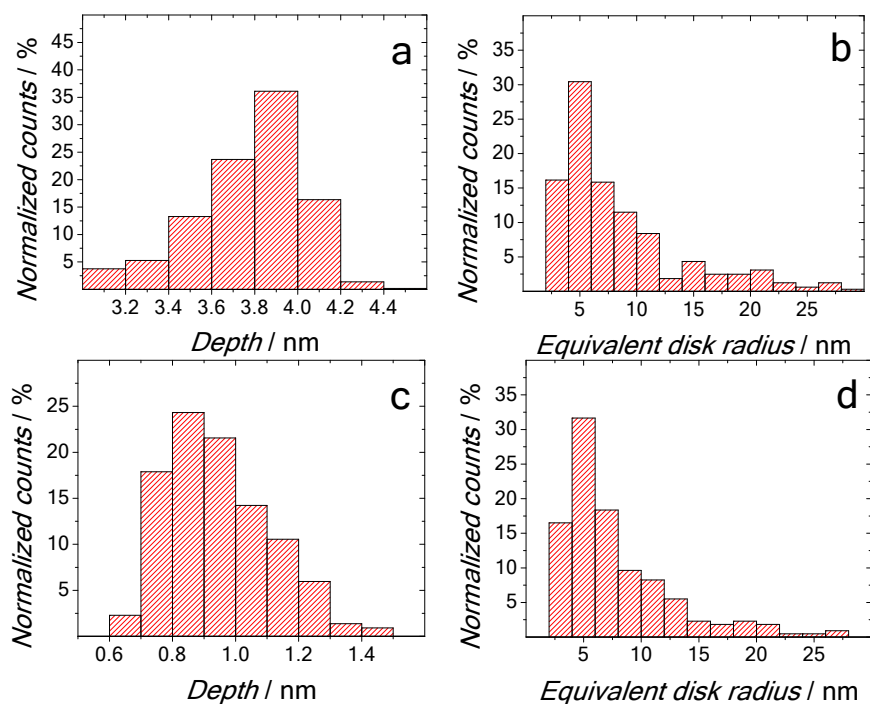


**Figure S4.** (a) The depth of pores and (b) the equivalent disk radius of the A $\beta$ O clusters surrounding the pores in BLM-A $\beta$ O<sub>s</sub>, deposited on a mica substrate and then imaged in the PBS (0.01 M phosphate buffer, 0.0027 M KCl, and 0.137 M NaCl, pH = 7.4) solution. (c) The depth and (d) equivalent disk radius of the defects in BLM-A $\beta$ O<sub>s</sub>-K162 deposited on a mica substrate and then imaged in the PBS (0.01 M phosphate buffer, 0.0027 M KCl, and 0.137 M NaCl, pH = 7.4) solution.

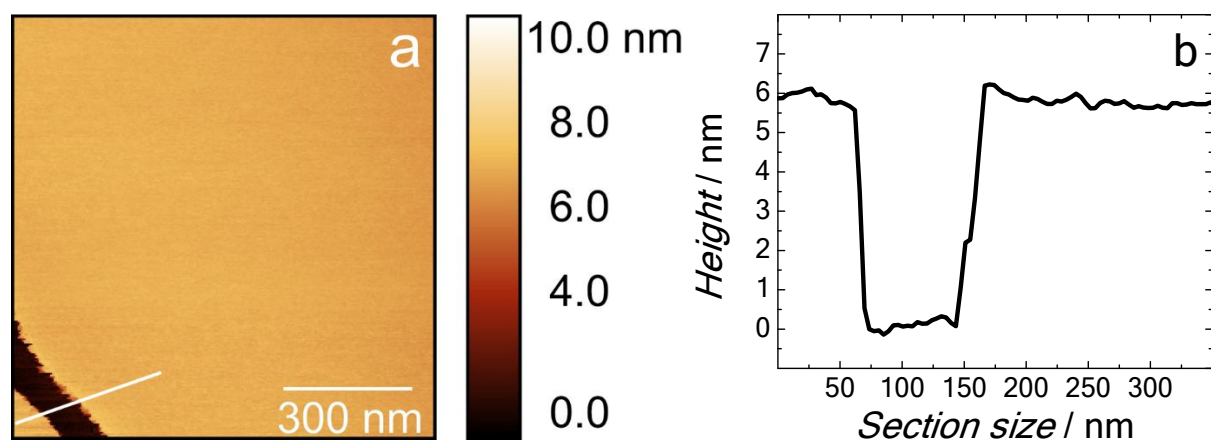


**Figure S5.** (a) The AFM topography image and (b) the corresponding cross-sectional profile of BLM in the presence of K162 in the PBS (0.01 M phosphate buffer, 0.0027 M KCl, and 0.137 M NaCl, pH = 7.4) solution at room temperature.

**Table S2.** The population of different A $\beta$  forms during 48 h of A $\beta$  aggregation.

Aggregation time, h	A $\beta$ monomers, %		A $\beta$ dimers, %		A $\beta$ tetramers, %		A $\beta$ octamers, %	
	no K162	K162	no K162	K162	no K162	K162	No K162	K162
0	47	58	10	12	9	6	3	2
24	19	44	6	6	12	12	12	4
48	6	12	6	16	20	13	3	6

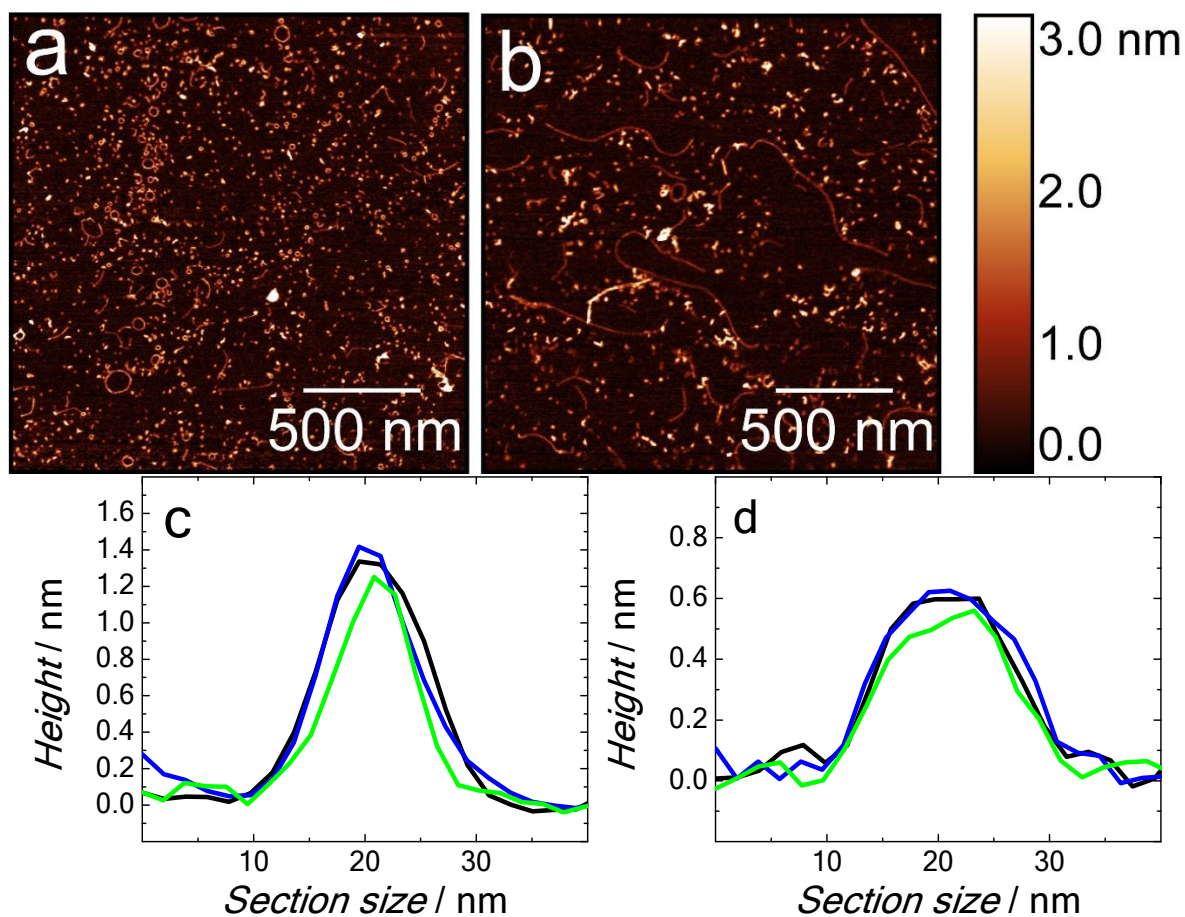


**Figure S6.** The AFM imaged topography of elongated Aβ aggregates formed in the (a) absence and (b) presence of K162 after 48 h of Aβ aggregation. Individual cross-sectional profiles measured along lines are shown in (c) Figure 4a and (d) 4b.

**Table S3.** Binding energies of interactions of A $\beta$  with K162 calculated from the molecular dynamics simulations with explicit solvent and implicit-solvent post-processing using the MMPBSA method.

System	Binding energy (kJ/mol)
K162 – K162	-5.72 $\pm$ 0.21
K162 – A $\beta$ M	-9.96 $\pm$ 0.16
K162 – A $\beta$ D	-15.71 $\pm$ 0.21
K162 – A $\beta$ F	-7.71 $\pm$ 0.28
A $\beta$ M – A $\beta$ M (in the absence of K162)	-103.94 $\pm$ 0.93
A $\beta$ D – A $\beta$ D (in the absence of K162)	-79.73 $\pm$ 1.30
A $\beta$ F – A $\beta$ F (in the absence of K162)	-123.71 $\pm$ 1.54
A $\beta$ M – A $\beta$ M (in the presence of K162)	4.63 $\pm$ 0.01
A $\beta$ D – A $\beta$ D (in the presence of K162)	73.65 $\pm$ 2.02
A $\beta$ F – A $\beta$ F (in the presence of K162)	26.79 $\pm$ 1.34

## References

- (1) Kastantin, M.; Ananthanarayanan, B.; Karmali, P.; Ruoslahti, E.; Tirrell, M. Effect of the Lipid Chain Melting Transition on the Stability of DSPE-PEG (2000) Micelles. *Langmuir* **2009**, *25* (13), 7279–7286. <https://doi.org/10.1021/la900310k>.
- (2) Biltonen, R. L.; Lichtenberg, D. The Use of Differential Scanning Calorimetry as a Tool to Characterize Liposome Preparations. *Chem. Phys. Lipids* **1993**, *64*, 129–142. [https://doi.org/10.1016/0009-3084\(93\)90062-8](https://doi.org/10.1016/0009-3084(93)90062-8).
- (3) Konyakhina, T. M.; Wu, J.; Mastroianni, J. D.; Heberle, F. A.; Feigenson, G. W. Phase Diagram of a 4-Component Lipid Mixture: DSPC/DOPC/POPC/Chol. *Biochim. Biophys. Acta - Biomembr.* **2013**, *1828*, 2204–2214. <https://doi.org/10.1016/j.bbamem.2013.05.020>.
- (4) Heberle, F. A.; Wu, J.; Goh, S. L.; Petruzielo, R. S.; Feigenson, G. W. Comparison of Three Ternary Lipid Bilayer Mixtures: FRET and ESR Reveal Nanodomains. *Biophys. J.* **2010**, *99*, 3309–3318. <https://doi.org/10.1016/j.bpj.2010.09.064>.
- (5) Ackerman, D. G.; Feigenson, G. W. Lipid Bilayers: Clusters, Domains and Phases. *Essays Biochem.* **2015**, *57*, 33–42. <https://doi.org/10.1042/BSE0570033>.